# Symmetry breaking for ratchet transport in the presence of interactions and a magnetic field

L. Ermann
*Departamento de Física Teórica, GIyA, Comisión Nacional de Energía Atómica, Buenos Aires, Argentina and Laboratoire de Physique Théorique du CNRS, IRSAMC, Université de Toulouse, UPS, F-31062 Toulouse, France*

A. D. Chepelianskii
*Cavendish Laboratory, Department of Physics, University of Cambridge, Cambridge CB3 0HE, United Kingdom*

D. L. Shepelyansky
*Laboratoire de Physique Théorique du CNRS, IRSAMC, Université de Toulouse, UPS, F-31062 Toulouse, France*
(Received 19 November 2012; published 21 February 2013)

We study the microwave induced ratchet transport of two-dimensional electrons on an oriented semidisk Galton board. The magnetic field symmetries of ratchet transport are analyzed in the presence of electron-electron interactions. Our results show that a magnetic field asymmetric ratchet current can appear due to two contributions, a Hall drift of the rectified current that depends only weakly on electron-electron interactions and a breaking of the time reversal symmetry due to the combined effects of interactions and magnetic field. In the latter case, the asymmetry between positive and negative magnetic fields vanishes in the weak interaction limit. We also discuss the recent experimental results on ratchet transport in asymmetric nanostructures.

DOI: 10.1103/PhysRevE.87.022912 PACS number(s): 05.45.Ac, 72.40.+w, 73.63.−b

## I. INTRODUCTION

The appearance of a directed flow induced by a zero-mean monochromatic force is a generic nonequilibrium phenomenon known as the ratchet effect (see, e.g., [1–3]). The ratchet transport at the nanoscale has attracted significant interest in recent years (see [4] and references therein). The electron ratchet currents induced by a monochromatic *ac* driving have been experimentally observed in asymmetric mesoscopic structures at high [5], very low [6], and gigahertz [7] frequencies. In the later experiments the ratchet effect was visible even at room temperatures, but these experiments lacked a detailed analysis of magnetic field resonance effects, typical of a two-dimensional electron gas (2DEG) in a magnetic field [8,9], and a dependence study of the ratchet current on microwave polarization. We note that the presence of resonances in a resistivity dependent on magnetic field and polarization dependence of ratchet transport ensure that a voltage induced by a microwave radiation appears to be due to an asymmetry of lattice structure and not due to other asymmetries potentially present in experimental devices.

The theoretical studies of 2DEG deterministic ratchet transport on a semidisk Galton board started in Ref. [10] and were further extended in Refs. [11–14]. The theoretical studies show that the ratchet effect exists not only for 2DEG but also for electrons in graphene plane with an oriented semidisk lattice [15]. The numerical simulations and analytical theory developed in Refs. [10–15] have been done for noninteracting electrons. They established that a directed chaotic deterministic ratchet transport emerges in such asymmetric nanostructures due to microwave radiation. The direction of the ratchet current can be controlled by the radiation polarization. The theoretical studies show that the ratchet effect also exists in the presence of moderate and strong interactions between electrons [16].

The theoretical works inspired the detailed experimental studies of the chaotic deterministic ratchet 2DEG transport on the semidisk Galton board of antidots performed by the Grenoble group [17]. These experiments clearly demonstrated the existence of ratchet transport in a high mobility 2DEG based on AlGaAs/GaAs heterojunctions with a semidisk array. The polarization dependence of ratchet current is found to be in qualitative agreement with the theory dependence for noninteracting electrons. It is also experimentally shown [17] that the ratchet is absent in arrays with circular antidots, ensuring that the effect is produced by semidisks and not by always present device asymmetries. More recently, the Grenoble group performed ratchet experiments with 2DEG in Si/SiGe heterostructures [18,19] where the interaction effects between electrons are expected to play a more important role [14]. The characteristic feature of these experiments is the dependence of ratchet transport on a magnetic field in the presence of interactions. Thus it is important to understand the properties of the ratchet of interacting particles in a magnetic field which creates a symmetry breaking in space and time. We note that previously the theoretical investigations were done only for noninteracting electrons in a magnetic field [12,14] or for interacting electrons without magnetic field [16]. Thus in this work we perform a more general study analyzing the properties of ratchet transport in the presence of interactions and magnetic field.

Indeed, an applied magnetic field induces a chiral movement of charge in a conducting sample. This chirality may be revealed in optical measurements such as the Faraday effect [20,21]. An emergence of a static magnetization due to an *ac* electric field is known as the inverse Faraday effect (see, e.g., [22]). Hence one can expect that transport properties of a chiral structure will strongly depend on the sign of the magnetic field. However, this argument, based on spatial symmetries, should also take into account that the equilibrium transport measurements are also constrained by the time reversal symmetry that implies Onsager-Casimir reciprocity relations [23,24]. Due to these relations a two-terminal conductance is always symmetric with the magnetic field masking the chirality. However, since the time reversal symmetry is valid only for equilibrium samples, it can be destroyed for measurements in a nonlinear transport regime. The appearance of magnetic field asymmetry in a nonlinear two-terminal transport has attracted significant theoretical and experimental attention in the mesoscopic physics community. Indeed, a microscopic disorder potential has no symmetry, and the absence of self-averaging in coherent samples makes such investigations possible. Surprisingly, even if all symmetries are broken in the out of equilibrium regime, theoretical calculations predict that interactions are required to observe a magnetic field antisymmetric component in nonlinear conductance. While measurements on coherent samples seem to support these predictions, measurements on samples with artificial asymmetric structures may produce asymmetric (or even antisymmetric) nonlinear transport even in regimes where interactions do not seem to play a role (for, e.g., high density) [17,25]. Thus, the investigations of ratchet transport in the presence of interactions and magnetic field will allow us to analyze the Onsager-Casimir reciprocity relations in a new frame.

In order to gain a deeper insight on the symmetry properties of nonlinear transport, we investigate numerically an interacting 2DEG with a periodic array of asymmetric (semidisk) antidots oriented in a preferential direction using the square lattice of oriented semidisks discussed in Refs. [15,16]. In this model a semidisk of radius $r_d$ is placed in a square of size $R$, and then this square covers periodically the whole $(x,y)$ plane (see inset of Fig. 1). We consider a homogeneous monochromatic linearly polarized electric field $\mathbf{E} = E_o \cos \omega t (\cos\theta, \sin\theta)$. This field creates a rectified current flow due to the asymmetric structure of the antidot superlattice. The direction of the flow can be controlled by the polarization of the microwave field and by a magnetic field perpendicular to the 2DEG plane.

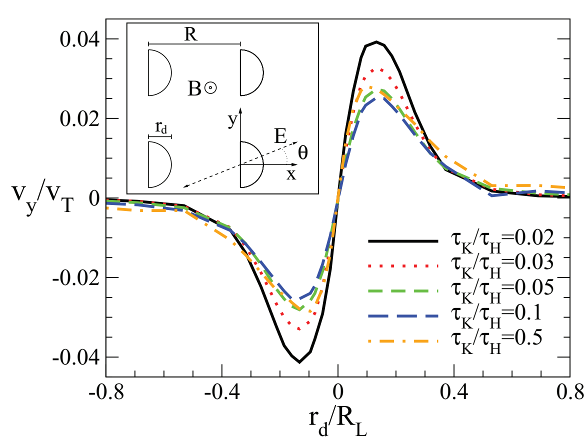


FIG. 1. (Color online) Dimensionless average ratchet velocity $v_y/v_T$ in the $y$ direction as a function of magnetic field $B$ given by dimensionless parameter $r_d/R_L \propto B$. The electric field is linearly polarized in the $y$ axis ($\theta = \pi/2$) with amplitude and frequency $E_0 = 0.1$ and $\omega = 0.1$, and the temperature of the Hoover thermostat is $T = 1$ with $\tau_H = 10$. The interactions between electrons go from a strong interaction regime ($\tau_K/\tau_H = 0.02$) to weak interactions ($\tau_K/\tau_H = 0.5$), as shown in the legend. The inset shows the directions of the electric and magnetic fields in a general case and the distribution of a semidisk periodic array with an orientation direction in the $x$ axis. The geometric ratio is fixed at $R/r_d = 4$, as shown in the inset.

The quantitative description of the ratchet current can be obtained on the basis of kinetic theory [14]. However, this theory rapidly breaks down in the presence of a magnetic field since it does not capture the particle dynamics when the cyclotron radius becomes of the order of the antidot radius. Moreover it was shown recently [16] that interactions could strongly modify the rectified current; hence this system allows us to investigate in detail the role of interactions on the magnetic field symmetry properties of the nonlinear response. In fact, we show that the antisymmetric component of the rectified current can be split into two terms. One term is weakly dependent on interactions and can be interpreted as a Hall drift of the rectified current in the preferential direction fixed by the semidisk superlattice. The second term vanishes in the absence of interactions, as predicted by theory [26–28]. Hence, depending on the measurement geometry, the antisymmetric component of the rectified current may vanish or not in absence of interactions.

## II. MODEL DESCRIPTION AND RESULTS

In this work we consider a 2DEG with elastic semidisk scatterers of radius $r_d$, oriented in direction $\mathbf{e}_x = \mathbf{x}$, and placed in a periodic square lattice of size $R \times R$ (see inset of Fig. 1). The electron motion is affected by an electric microwave field $\mathbf{E}\cos\omega t = E_0(\cos\theta, \sin\theta, 0)\cos\omega t$ linearly polarized at angle $\theta$ to $\mathbf{e}_x$ and a transverse, uniform, and constant magnetic field $\mathbf{B} \propto \mathbf{e}_z/R_L$ (inversely proportional to the Larmor radius $R_L$). The system also interacts with a Nosé-Hoover thermostat which equilibrates the ensemble of particles to the Boltzmann distribution with temperature $T = mv_T^2/2$ in a characteristic time $\tau_H$ (see, e.g., [29]). The electron interactions are treated in the frame of the mesoscopic multiparticle collision model proposed by Kapral (see, e.g., [30]). The method consists of dividing the coordinate space of each square of size $R \times R$ with $N$ particles in $N_{\rm cel}$ collision cells. Inside each cell the collisions are modeled by a rotation of all particle velocities on a random angle in the moving center-of-mass frame, preserving the total momentum and energy of the system. These rotations occur with a repetition period given by a characteristic time $\tau_K$. In this way large and small values of $\tau_K$ correspond to weak and strong interactions, respectively. In this work we follow our previous studies of interaction effects on ratchet transport [16], where the interactions were treated in the frame of the Kapral approach.

We fix the geometric ratio $R/r_d = 4$ in order to work at low antidot density and to avoid geometrical particularities, which may exist for $R/r_d \simeq 1$. The number of particles is fixed at $N = 10^4$, and for numerical simulations we choose dimensionless parameters $T = 1$, $r_d = 1$, $\tau_H = 10$, and electron charge and mass $e = m_e = 1$. The Kapral grid for interactions is fixed to have $N_{\rm cel} = 100 \times 100$ cells in the whole space region $R^2$. Therefore the only parameter controlling the interaction strength is the inverse Kapral time $1/\tau_K$. This choice of parameters is similar to those used in Ref. [16]. We recall that $\tau_H$ determines the relaxation time to the equilibrium.

The steady-state net current of the system is proportional to the average particle velocities. This current can be described as a vector $\mathbf{j}$ split into two components of different magnetic field symmetries: $\mathbf{j} = \mathbf{j}_s + \mathbf{j}_a$, where $\mathbf{j}_s$ are symmetric and $\mathbf{j}_a$ are antisymmetric components. These two vectors depend quadratically on the alternating electric field amplitude $\mathbf{E}$ and can also depend on $\mathbf{e}_x$ and $\mathbf{B}$; therefore their most general expression reads

$$\begin{aligned}\mathbf{j}_s &= f_1(B)(\mathbf{e}_x \cdot \mathbf{E})\mathbf{E} + f_2(B)\mathbf{E}^2\mathbf{e}_x,\\ \mathbf{j}_a &= g_1(B)(\mathbf{e}_x \cdot \mathbf{E})(\mathbf{B} \wedge \mathbf{E}) + g_2(B)\mathbf{E}^2(\mathbf{B} \wedge \mathbf{e}_x).\end{aligned} \tag{1}$$

Here $f_i(B), g_i(B)$ $(i = 1,2)$ are functions of the modulus of the magnetic field $B = |\mathbf{B}|$ depending implicitly on the rest of the model parameters. Specifically, we focus on the dependence of the antisymmetric component of the current on the strength of interactions between electrons.

We note that both terms in the second line of Eq. (1) can be decoupled for different values of $\theta$. For the electric and magnetic fields used in this model, the dimensionless velocity can be written as

$$\begin{aligned}\frac{v_x(\theta)}{v_T} &= \frac{E_0^2}{\sqrt{2T}}\left[\tilde{f}_1 \cos^2\theta + \tilde{f}_2 - \frac{\tilde{g}_1 \sin 2\theta}{2}\right],\\ \frac{v_y(\theta)}{v_T} &= \frac{E_0^2}{\sqrt{2T}}\left[\frac{\tilde{f}_1 \sin 2\theta}{2} + \tilde{g}_1\cos^2\theta + \tilde{g}_2\right],\end{aligned} \tag{2}$$

where $\tilde{f}_i$ and $\tilde{g}_i$ $(i = 1,2)$ are symmetric and antisymmetric functions of the magnetic field in the $\mathbf{z}$ direction (or the related Larmor radius $R_L = v_T/B$). These functions are proportional to the functions in Eqs. (1), $\tilde{f}_i \propto f_i(B)$ and $\tilde{g}_i \propto g_i(B)/R_L$ (where we take $R_L > 0$ and $R_L < 0$ for the magnetic field in the $\mathbf{z}$ and $-\mathbf{z}$ directions, respectively). Following Eqs. (2), we can note that for $\theta = 0$ and $\theta = \pi/2$, velocities in the $x$ direction are symmetric, while the $y$ components are antisymmetric.

In the case of a polarized electric field in the $y$ direction $(\theta = \pi/2)$, $v_y$ can be asymmetric in the magnetic field only due to the second term in the second equation in (2), denoted $\tilde{g}_2$. This case is illustrated in Fig. 1 for the dimensionless quantities $v_y/v_T$ plotted versus $r_d/R_L$ at different values of Kapral time $\tau_K$ and for the rest of the parameters specified in the caption. The data in Fig. 1 show that the dependence of the ratchet velocity $v_y/v_T$ is an asymmetric function of $r_d/R_L \propto B$ with a maximum of $|v_y|$ at $r_d/R_L \approx \pm 0.15$. The amplitude of this maximum increases by a factor 2 with the increase of interactions (decrease of $\tau_K$).

Following the first line of Eq. (2), the asymmetry given by $\tilde{g}_1$ can be analyzed via the parameter dependence of $v_x/v_T$ at small angles of linear polarization of electric field directed along both $\mathbf{x}$ and $\mathbf{y}$. The emergence of $\tilde{g}_1$ from a symmetric behavior in the magnetic field is shown in the top panel of Fig. 2 for $v_x/v_T$ with small values of $\theta$ in the strong interaction regime $(\tau_K/\tau_H = 0.02)$. In the case of $\theta = \pi/20$, the bottom panel of Fig. 2 shows the behavior of asymmetry in $v_x/v_T$ for different interaction times, going from $\tau_K/\tau_H = 0.02$ to $\tau_K/\tau_H = 0.5$. The striking feature of the bottom panel of Fig. 2 is that the asymmetry in the magnetic field is rather strong for strong interactions, while in the limit of weak interactions the asymmetry completely disappears and we recover the symmetric curve as a function of the magnetic field.

A deeper analysis of the symmetry properties can be done by considering the flux of velocities in coordinate space. It is known that for interacting particles the average velocity behavior can be rather complex with the emergence of some vortices [16]. In Fig. 3 we present the velocity flux for weak and strong interaction regimes with positive and negative magnetic fields. The analyzed values of the Larmor radius correspond to the relative minima of $v_x/v_T$ marked with arrows in Fig. 2 at negative and positive values of $r_d/R_L$. Figure 3 shows the flow structure at $r_d/R_L \simeq 0.16$ (top panels) and at $r_d/R_L \simeq -0.1$ (bottom panels). The polarization angle in the four panels is fixed at $\theta = \pi/20$, and therefore the reflection symmetry $y \to -y$ is not preserved. The data show that the vortex asymmetric structure is more pronounced in the case of strong interactions, shown in the right panels.

The polarization dependence of the ratchet current in the $x$ direction is analyzed in Fig. 4. We see that even for various magnetic fields the dependence on polarization angle $\theta$ is essentially symmetric at weak interactions (top panel), while for strong interactions (bottom panel) we have a strongly asymmetric behavior at moderate magnetic fields $(r_d/R_L = 0.053, 0.133)$. At a relatively large magnetic field $(r_d/R_L = 0.53)$ the amplitude of the ratchet current becomes rather small since the Larmor radius becomes smaller than the distance between semidisks. Thus the data in Fig. 4 also show that the asymmetry of the ratchet transport appears only in the presence of interactions.

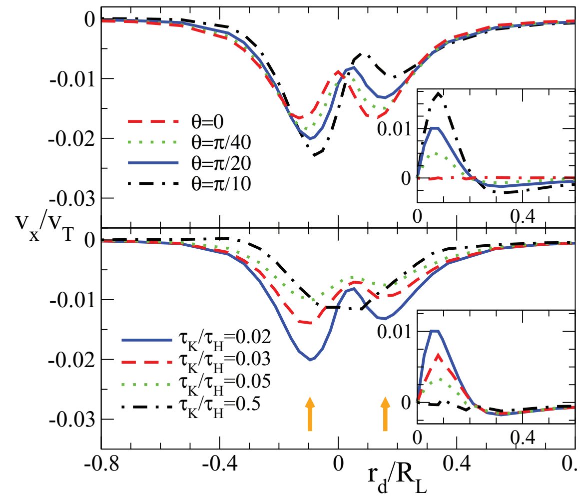


FIG. 2. (Color online) Dimensionless average ratchet velocity in the $x$ direction $(v_x/v_T)$ as a function of magnetic field. The top panel shows the strong interaction regime (with $\tau_K/\tau_H = 0.02$) for the rest of the parameters specified in the caption of Fig 1. The electrical field is polarized near the $x$ axis, where the dashed red curve represents the symmetrical case of $\theta = 0$. The small deviation angles are shown at $\theta = \pi/40$ by a dotted green curve, $\theta = \pi/20$ by a solid blue curve, and $\theta = \pi/10$ by a dot-dashed black curve. The bottom panel shows the case of fixed polarization angle $\theta = \pi/20$ and different strengths of interactions between particles. The interaction times are $\tau_K/\tau_H = 0.02$ (solid blue curve), $\tau_K/\tau_H = 0.03$ (dashed red curve), $\tau_K/\tau_H = 0.1$ (dotted green curve), and $\tau_K/\tau_H = 0.5$ (dot-dashed black curve). The inserts in both panels show the dimensionless asymmetry $[v_x(r_d/R_L) - v_x(-r_d/R_L)]/v_T$ as a function of $r_d/R_L$ for the same parameters as in the main panel, using the same color scheme. Orange arrows show the values of the magnetic field analyzed in Fig. 3.

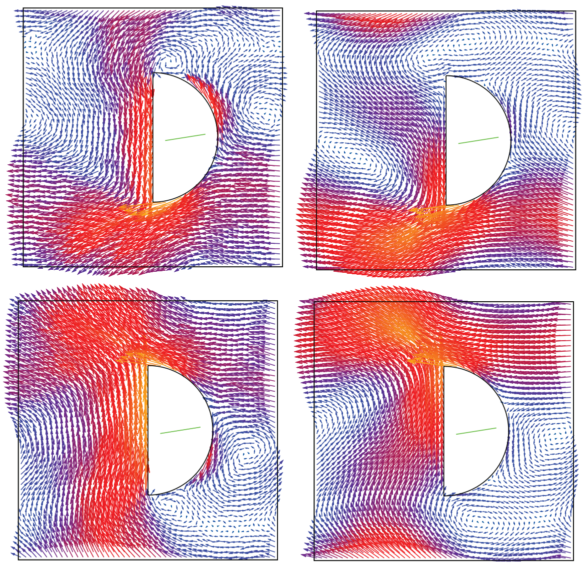

FIG. 3. (Color online) Map of local averaged velocities in $(x,y)$ with $x,y \in [-2,2)$ and linear polarized electrical field $\theta = \pi/20$ [shown by the green (light gray) line inside the semidisk scatterer]; other parameters are the same as in Fig. 1 (here $x,y$ are expressed in units of disk radius $r_d$, the bounding square marks the size of the periodic lattice cell). The left panels show the cases of weak interactions between particles at $\tau_K/\tau_H = 0.5$, while the right panels show the strong interaction regime at $\tau_K/\tau_H = 0.02$. The values of the magnetic field are given by $r_d/R_L = 0.1591$ in the top panels and $r_d/R_L = -0.0955$ in the bottom panels [indicated with orange (gray) arrows in Fig. 2]. The velocities are shown by arrows whose size is proportional to the velocity amplitudes, which is also indicated by color [from yellow (light gray) for large to blue (dark gray) for small amplitudes].

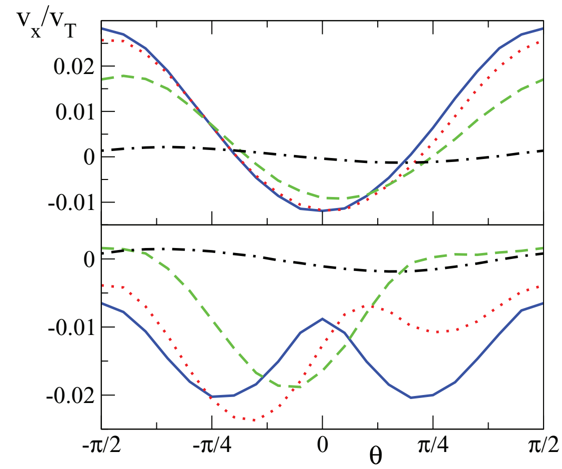


FIG. 4. (Color online) Polarization dependence of $x$-component of the averaged ratchet velocity $v_x/v_T$, for weak interactions between particles in top panel ($\tau_K/\tau_H = 0.5$), and for strong interactions in bottom panel ($\tau_K/\tau_H = 0.02$). Four different values of magnetic fields are shown in both panels: zero magnetic field ($r_d/R_L = \infty$, solid blue curve), $r_d/R_L = 0.053$ by dotted red curve, $r_d/R_L = 0.133$ by dashed green curve and $r_d/R_L = 0.53$ by dot-dashed black curve. Here the angle $\theta$ is measured in radians.

## III. DISCUSSION

In this work we study the symmetry properties of the ratchet transport on an oriented semidisk antidot superlattice. We show that while the ratchet flow on the oriented semidisk superlattice (along the $x$ axis) does not depend on the sign of the magnetic field for a noninteracting 2DEG, interactions can give rise to an antisymmetric component of the flow in the semidisk direction as a function of the magnetic field. This result is consistent with the case of mesoscopic samples where deviations from Onsager-Casimir reciprocity relations were shown to occur only in the presence of electron-electron interactions [26–28]. On the contrary, the flow perpendicular to the semidisk direction ($y$ axis) is asymmetric even when interactions are absent. We argue that the origin of this component of the flow is a Hall drift of the rectified current. This contribution is absent in disordered mesoscopic samples because the translational symmetry is broken by a disorder potential where no preferential direction is present for the flow.

The comparison with Refs. [17–19] highlights various aspects of these skillful experiments. At weak electron-electron interactions typical of AlGaAs/GaAs heterojunctions [17] there is a qualitative agreement between the theory and experiment on polarization dependence and approximately symmetric current response to sign change of the magnetic field, even if the absolute quantitative values differ from theoretical predictions (see [16] for a more detailed discussion). For experiments with Si/SiGe heterostructures [18,19] the effects of the interactions are stronger, and an asymmetric response in the magnetic field is clearly observed in experiments (see, e.g., Fig. 3 in Ref. [18]). In this case the change of polarization from $\theta = 0$ to $\theta = \pi/2$ does not change the sign of photovoltage that also appears in theoretical models at strong interactions, as discussed in Ref. [16]. Also the ratchet effect is clearly suppressed in experiment and theory at large magnetic fields. However, at the same time there are significant differences between experiments [18,19] and the theoretical results presented here. Indeed, for $\theta = \pi/2$ the theory predicts a change of the photovoltage sign upon inversion of the magnetic field (see Fig. 1), while there is no such sign change in experiments (see, e.g., Fig. 3 in Refs. [18] and [19]). It is possible that a finite sample size leads to a certain charge accumulation in the experimental setup (see indications for that in Fig. 4 in Ref. [19]), which may explain the difference with the theory where the analysis is done for an infinite lattice size. We should also note that the present studies were done for a square lattice of semidisks, while the experiments [17–19] were performed on a hexagonal lattice of semidisks. However, in both cases the density of the semidisks is relatively low (since $R/r_d = 4$ here and $R/r_d \approx 5$ in Refs. [18,19]). Thus, the ratchet transport is created mainly by scattering on a one semidisk (see discussion in Ref. [14]), and the difference between square and hexagonal lattices is not expected to be important.

Finally, we note that the electron-electron interactions are treated here in the frame of the Kapral approach, which corresponds to the Boltzmann distribution typical for relatively large temperatures. At low temperatures, with $k_B T$ being small compared to the Fermi energy $E_F$, one should model both the Fermi-Dirac distribution and interactions. The Fermi-Dirac distribution can be modeled by the Metropolis approach used in Refs. [12,14], but the treatment of interactions in this Fermi-Dirac regime remains an important challenge for numerical simulations. It is possible that modeling real experiments with interactions and the Fermi-Dirac statistical distribution will produce a better agreement between numerical simulations and experimental results. The discussed comparison between the present theoretical studies and the most advanced experiments reported in Refs. [17–19] shows that the further experimental and theoretical research on the electron ratchet transport in asymmetric nanostructures with dynamical chaos represents significant fundamental scientific interest.

## ACKNOWLEDGMENTS

We thank M. L. Polianski for fruitful discussions regarding out of equilibrium transport in mesoscopic systems. This work was supported in part by the French PNANO ANR project NANOTERRA, and one of us (A.D.C.) acknowledges support from St Catharine's College.

[1] J. Jülicher, A. Ajdari, and J. Prost, Rev. Mod. Phys. **69**, 1269 (1997).
[2] R. D. Astumian and P. Hänggi, Phys. Today **55**(11), 33 (2002).
[3] P. Reimann, Phys. Rep. **361**, 57 (2002).
[4] P. Hänggi and F. Marchesoni, Rev. Mod. Phys. **81**, 387 (2009).
[5] A. Lorke, S. Wimmer, B. Jager, J. P. Kotthaus, W. Wegscheider, and M. Bichler, Phys. B **249–251**, 312 (1998).
[6] H. Linke, T. E. Humphrey, A. Löfgren, A. O. Sushkov, R. Newbury, R. P. Taylor, and P. Omling, Science **286**, 2314 (1999).
[7] A. M. Song, P. Omling, L. Samuelson, W. Seifert, I. Shorubalko, and H. Zirath, Appl. Phys. Lett. **79**, 1357 (2001).
[8] D. Weiss, M. L. Roukes, A. Menschig, P. Grambow, K. von Klitzing, and G. Weimann, Phys. Rev. Lett. **66**, 2790 (1991).
[9] G. M. Gusev, Z. D. Kvon, V. M. Kudryashov, L. V. Litvin, Y. V. Nastaushev, V. T. Dolgopolov, and A. A. Shashkin, Pis'ma Zh. Eksp. Teor. Fiz. **54**, 369 (1991) [JETP Lett. **54**, 364 (1991)].
[10] A. D. Chepelianskii and D. L. Shepelyansky, Phys. Rev. B **71**, 052508 (2005).
[11] G. Cristadoro and D. L. Shepelyansky, Phys. Rev. E **71**, 036111 (2005).
[12] A. D. Chepelianskii, Eur. Phys. J. B **52**, 389 (2006).
[13] M. V. Entin and L. I. Magarill, Phys. Rev. B **73**, 205206 (2006).
[14] A. D. Chepelianskii, M. V. Entin, L. I. Magarill, and D. L. Shepelyansky, Eur. Phys. J. B **56**, 323 (2007).
[15] L. Ermann and D. L. Shepelyansky, Eur. Phys. J. B **79**, 357 (2011).
[16] A. D. Chepelianskii, M. V. Entin, L. I. Magarill, and D. L. Shepelyansky, Phys. Rev. E **78**, 041127 (2008).
[17] S. Sassine, Yu. Krupko, J.-C. Portal, Z. D. Kvon, R. Murali, K. P. Martin, G. Hill, and A. D. Wieck, Phys. Rev. B **78**, 045431 (2008).
[18] I. Bisotto, E. S. Kannan, R. Murali, T. J. Beck, L. Jalabert, and J.-C. Portal, Nanotechnology **22**, 245401 (2011).
[19] E. S. Kannan, I. Bisotto, J.-C. Portal, R. Murali, and T. J. Beck, Appl. Phys. Lett. **98**, 193505 (2011).
[20] M. Faraday, *Faraday's Diary*, Vol. 4, *Nov 12, 1839 - June 26, 1947*, edited by Th. Martin (Bell, London, 1933).
[21] L. D. Landau and E. M. Lifshitz, *Electrodynamics of Continuous Media* (Pergamon, New York, 1960).
[22] M. L. Polianski, Phys. Rev. B **80**, 241301(R) (2009).
[23] L. Onsager, Phys. Rev. **37**, 405 (1931); **38**, 2265 (1931).
[24] H. B. G. Casimir, Rev. Mod. Phys. **17**, 343 (1945).
[25] A. D. Chepelianskii and H. Bouchiat, Phys. Rev. Lett. **102**, 086810 (2009).
[26] D. Sánchez and M. Büttiker, Phys. Rev. Lett. **93**, 106802 (2004).
[27] B. Spivak and A. Zyuzin, Phys. Rev. Lett. **93**, 226801 (2004).
[28] M. L. Polianski and M. Büttiker, Phys. Rev. Lett. **96**, 156804 (2006).
[29] W. G. Hoover, *Time Reversibility, Computer Simulation, and Chaos* (World Science, Singapore, 1999).
[30] A. Malevanets and R. Kapral, in *Novel Methods in Soft Matter Simulations*, edited by M. Karttunens, I. Vattulainen, and A. Lukkarinen, Lecture Notes in Physics, Vol. 640 (Springer, Berlin, 2004), p. 116.